Two dimensional shot-profile migration data reconstruction

Sam T. Kaplan, University of Alberta, Mostafa Naghizadeh, University of Calgary, and Mauricio D. Sacchi, University of Alberta*

SUMMARY

We introduce *two dimensional shot-profile migration data reconstruction* (SPDR2). SPDR2 reconstructs data using least-squares shot-profile migration with a constant migration velocity model. The velocity model is chosen both for efficiency and so that minimal assumptions are made about earth structure. At the core of least-squares migration are forward (de-migration) and adjoint (migration) operators, the former mapping from model space to data space, and the latter mapping from data space to model space. SPDR2 uses least-squares migration to find an optimal model which, in turn, is mapped to data space using de-migration, providing a reconstructed shot gather. We apply SPDR2 to real data from the Gulf of Mexico. In particular, we use SPDR2 to extrapolate near offset geophones.

INTRODUCTION

In seismic data reconstruction, algorithms tend to fall into one of two categories, being rooted in either signal processing or the wave equation. Examples of the former include Spitz (1991), Gülünay (2003), Liu and Sacchi (2004), Hennenfent and Herrmann (2006), and Naghizadeh and Sacchi (2007), while examples of the later include Stolt (2002), Chiu and Stolt (2002), Trad (2003), Ramírez et al. (2006), and Ramírez and Weglein (2009). SPDR2 belongs to the family of wave equation based methods for data reconstruction. It differs from previous efforts in its parameterization of model space, being based on shot-profile migration (e.g. Biondi, 2003) and de-migration operators. Additionally, it relies on data fitting methods such as those used in Trad (2003), rather than direct inversion and asymptotic approximation which are used in, for example, Stolt (2002).

A challenge in data reconstruction is alias. In particular, when aliased energy is present and interferes with signal, their separation becomes challenging (but, not impossible). A recent example of data reconstruction is Naghizadeh and Sacchi (2007). They use the non-aliased part of data to aid in the reconstruction of the aliased part of data. An alternative approach is to transform data via some operator that maps from data space to some model space, and such that in that model space, the corresponding representation of signal and alias are separable. This is a common approach in many signal processing methods, and is also the approach that we take in SPDR2. In particular, the SPDR2 model space is the sum of constant velocity shot-profile migrated gathers (i.e. a sum of common shot image gathers). This means that the SPDR2 model space is a representation of the earth's reflectors parameterized by pseudo-depth (i.e. depth under the assumption of a constant migration velocity model) and lateral position. We will show that under the assumption of limited dips in the earth's reflectors, the SPDR2 model space allows for the suppression of alias while preserving signal, thus allowing for the reconstruction of aliased data.

We begin with a description of shot-profile migration and de-migration built from the Born approximation to the acoustic wave-field and constant velocity Green's functions. We apply shot-profile migration to an analytic example in order to illustrate its mapping of signal and alias from data space (shot gathers) to model space (image gather). The mapping will infer that with constrained dip in the earth's reflectors, the signal and alias map to disjoint regions of model space. We note that if the dips in the earth's reflectors are large, then the model space representation of signal and alias are not necessarily disjoint, and the SPDR2 algorithm will fail unless survey parameters are adjusted to increase Nyquist geophone wave-numbers. Given the de-migration (forward) and migration (adjoint) operators, we construct a set of weighted least-squares normal equations for least-squares migration. The normal equations are built such that 1) to some prescribed noise tolerance, the reconstructed shot gathers fit the observed shot gathers, and 2) the aliased portion of model space is suppressed via model weights. Solving the normal equations gives an optimal common shot image gather, and, in turn, de-migration of the optimal common shot image gather gives reconstructed shot gathers. In total, this is the procedure followed in the SPDR2 method. We apply SPDR2 to a real data example from the Gulf of Mexico, where we extrapolate data to near offsets.

SHOT-PROFILE MIGRATION AND DE-MIGRATION OPERATORS

The shot-profile migration and de-migration operators are constructed from the Born approximation to the scalar wave equation using Green's functions constructed from a constant reference wave-speed c_0. In particular, the de-migration (i.e. forward) operator is,

$$\psi_s(\mathbf{x}_g,\omega,\mathbf{x}_{s(q)}) = \left(\frac{1}{2\pi}\right)^4 \left(\frac{\omega}{c_0}\right)^2 \mathscr{F}^* \int_{z_0}^{\infty} u_p(\mathbf{k}_{gx},z',\omega) \times \mathscr{F}\left[\mathscr{F}_s^* u_p(\mathbf{k}_{gx},z',\omega) g(\mathbf{k}_{gx},\mathbf{x}_{s(q)},\omega)\right] \alpha(\mathbf{x}_g,z') dz'. \tag{1}$$

and the migration (i.e. adjoint) operator is,

$$\begin{aligned}\alpha^{\dagger}(\mathbf{x}_g,z') = \left(\frac{1}{2\pi}\right)^4 \sum_{q=1}^{n_s} \int \left(\frac{\omega}{c_0}\right)^2 \\ \times \left[\mathscr{F}^* u_p^*(\mathbf{k}_{gx},z',\omega) g^*(\mathbf{k}_{gx},\mathbf{x}_{s(q)},\omega)\right] \\ \times \mathscr{F}^* u_p^*(\mathbf{k}_{gx},z',\omega) \mathscr{F}\psi_s(\mathbf{x}_g,\omega,\mathbf{x}_{s(q)}) d\omega.\end{aligned} \tag{2}$$

where,

$$u_p(\mathbf{k}_{gx},z',\omega) = -\frac{e^{ik_{gz}(z'-z_0)}}{i4k_{gz}}, \tag{3}$$

$$k_{gz} = sgn(\omega)\sqrt{\frac{\omega^2}{c_0^2} - \mathbf{k}_{gx}\cdot\mathbf{k}_{gx}}, \quad (4)$$

and,

$$g(\mathbf{k}_{gx},\mathbf{x}_s,\omega) = 2\pi f(\omega)e^{-i\mathbf{k}_{gx}\cdot\mathbf{x}_s}. \quad (5)$$

In equations 1-5, $\mathscr{F}$ is the two dimensional Fourier transform, mapping from lateral space $\mathbf{x}_g = (x_g, y_g)$ to lateral wave-numbers $\mathbf{k}_{gx} = (k_{gx}, k_{gy})$. We use symmetric $(1/\sqrt{2\pi})$ normalization factors in our Fourier transforms so that $\mathscr{F}^*$, the adjoint operator of $\mathscr{F}$, is also its corresponding inverse Fourier transform. The operator $\mathscr{F}_s^*$ is used to denote the inverse Fourier transform with the opposite Fourier convention (that is, $\mathscr{F}_s^* = \mathscr{F}$). This adopts the Fourier convention used in Clayton and Stolt (1981). The function u_p in equation 3 is a phase-shift operator, propagating the wave-field towards, or away from potential scattering points. In equation 3, the vertical wave-number k_{gz} is given by the dispersion relation in equation 4. Finally, $g(\mathbf{k}_{gx},\mathbf{x}_{s(q)},\omega)$ given by equation 5 is the Fourier representation of the q^{th} seismic point source located laterally at $\mathbf{x} = \mathbf{x}_{s(q)} = (x_{s(q)}, y_{s(q)})$. We assume that there are n_s sources.

OBSERVED DATA ON A NOMINAL GRID

SPDR2 reconstructs missing data in both geophone and shot dimensions. In the geophone dimension we assume some nominal and observed grid. We will assume a $2D$ problem so that $\mathbf{x}_g$ and $\mathbf{x}_{s(q)}$ simplify to, respectively, x_g and $x_{s(q)}$. For all shots, we let the nominal grid x_g^n be invariant to shot location $x_{s(q)}$. On the other hand, the observed grid necessarily varies with shot location due to the acquisition geometry of the seismic experiment so that for the q^{th} shot, we let $x_g^{o(q)}$ denote the observed grid. There is no analogous nominal grid for the shot dimension. That is, both the observed and reconstructed shots can be located arbitrarily along the shot dimension. The caveat being that the aperture of the common shot image gather corresponding to the reconstructed shot must be sufficiently illuminated by the observed shots. This caveat will be illustrated when we consider the reconstruction of missing near offset traces. We give a schematic representation of the nominal grid x_g^n for multiple shot locations in Figure 1. The empty and filled boxes in Figure 1 represent the nominal grid x_g^n, the black filled boxes represent the observed grid $x_g^{o(q)}$ (i.e. data traces), the gray filled circles represent the observed shot locations relative to the x_g axis, and the empty circle represents a shot location for SPDR2 to reconstruct relative to the geophone axis. Note that the shot locations need not fall on the nominal geophone grid.

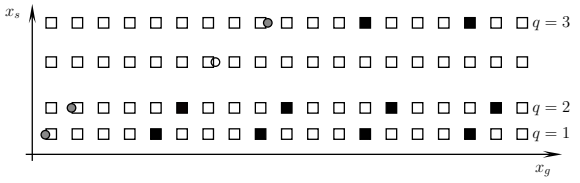

Figure 1: Schematic of the nominal and observed grids for SPDR2 The squares are the nominal grid, the black filled squares are the observed grid, and the gray filled circles are the observed shot locations. The empty circle represents a missing shot.

ADJOINT MAPPING OF SIGNAL AND ALIAS DUE TO THE OBSERVED GRID

We analyze the adjoint operator in equation 2 with an analytic example which, in turn, motivates weights for the least-squares normal equations used in the SPDR2 algorithm.

We let $\bar{\psi}_s(x_g,\omega,x_{s(q)}) = III_o(x_g)\psi_0(\omega)$ for $q = 1\ldots n_s$, where III_o is the sampling (Shah) function for the observed grid for all n_s shots. The Fourier transformed function $\bar{\psi}_s(k_{gx},\omega,x_{s(q)})$ is signal and alias in data space for the q^{th} shot. We are interested in their manifestation in model space. We substitute $\bar{\psi}_s(k_{gx},\omega,x_{s(q)})$ for $\mathscr{F}\psi_s(x_g,\omega,x_{s(q)})$ in the adjoint operator (equation 2) finding by way of the sampling theorem (e.g. Lathi, 1998),

$$\bar{\alpha}^\dagger(x_g,z) = \sum_p \int_{-\infty}^{\infty} \bar{\alpha}_p^\dagger(x_g,z,\omega)d\omega, \quad (6)$$

and where it can be shown that (letting $k = \omega/c_0$, $k_p = p2\pi/\Delta x_g^o$, and Δx_g^o define the observed grid spacing in III_o),

$$\bar{\alpha}_p^\dagger(k_{gx},k_z,\omega) = \frac{f^*(\omega)\psi_0(\omega)}{\Delta x_g^o}\left(\frac{\omega}{c_0}\right)^2 \sum_{q=1}^{n_s} e^{i(k_{gz}-k_p)x_{s(q)}} \times \delta\left(k_z + sgn(\omega)\left(\sqrt{k^2-k_p^2} + \sqrt{k^2-(k_{gx}-k_p)^2}\right)\right). \quad (7)$$

The term $\int \bar{\alpha}_0^\dagger(x_g,z,\omega)d\omega$ from equations 6 and 7 is the hypothetical image that would be obtained from a continuously sampled spatial dimension x_g in the data (i.e. $\bar{\alpha}_0^\dagger = \alpha^\dagger$), and $\bar{\alpha}_p^\dagger$, $p \neq 0$ is the expression of the alias in model space (i.e. the model space alias).

In the adjoint of the sampling function, we assume that $\bar{\alpha}_p^\dagger$ is band limited so that, equation 7 becomes,

$$\alpha_p^\dagger(k_{gx},k_z,\omega) = h(k_{gx},k_z)\bar{\alpha}_p^\dagger(k_{gx},k_z,\omega), \quad (8)$$

where,

$$h(k_{gx},k_z) = \begin{cases} 1 & , \quad |k_{gx}| \le k_b(k_z) \\ 0 & , \quad |k_{gx}| > k_b(k_z), \end{cases}$$

and where $k_b(k_z)$ is built from the expected maximum dip of the earth's reflectors, as represented in pseudo-depth. In particular, if a reflector has dip ξ such that,

$$\alpha(x_g,z) = \delta(z - \xi x_g),$$

then it can be shown that,

$$\alpha(k_{gx},k_z) = 2\pi\delta(k_{gx} + \xi k_z). \quad (9)$$

Hence, it must be that $k_b(k_z) = \xi k_z$. For example, when the dip of the reflector is null, so is k_b, and, likewise, k_b increases with increasing ξ. Figure 2 illustrates equations 7 and 8 for

small dip ($\xi = 0.1$), and five frequencies spaced evenly between 6 and $10Hz$. In Figure 2, we identify the model space signal ($p = 0$) and alias ($p = \pm 1, \pm 2$), and note that they are are separable. This is, in part, due to the band limiting function $h(k_{gx}, k_z)$ in equation 8, and will make it possible to build a data reconstruction algorithm that filters the alias $p \neq 0$, but preserves the signal $p = 0$.

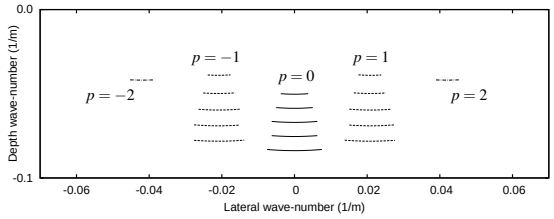

Figure 2: We represent the Dirac delta function in the adjoint of the sampling function (equation 7) under the band limitation constraint introduced in equation 8.

LEAST-SQUARES DATA RECONSTRUCTION

To construct the weighted least-squares inversion, we begin with some definitions. We let $\mathbf{d}$ be a data vector of length M realized from n_s observed shot gathers $\psi_s(x_g^n, \omega, x_{s(q)})$ so that $M = n_s n_\omega n_g^n$, and where we recall that x_g^n describes the nominal grid (sampled with n_g points) for the lateral dimension x_g, and the forward and adjoint operators are evaluated for n_ω realizations of frequency. The data $\mathbf{d}$ will be nonzero only for the intersection of the nominal x_g^n and observed $x_g^{o(q)}$ grids. We let $\mathbf{m}$ be a model vector of length N realized from $\alpha(x_g^n, z)$, where $N = n_z n_g^n$, and n_z are the number of samples in depth for the shot-profile migration image gather. Last, we let $\mathbf{A}$ be the $M \times N$ matrix representation of the forward operator (shot-profile de-migration in equation 1), and $\mathbf{A}^H$ its corresponding adjoint operator (shot-profile migration in equation 2). Then, $\mathbf{A}$ maps from $\mathbf{m}$ to $\mathbf{d}$.

To find an optimal $\mathbf{m}$ that honours the observed data $\mathbf{d}$, we find the minimum of the cost function,

$$\begin{aligned} \phi(\mathbf{m}) &= ||\mathbf{W}_d(\mathbf{d} - \mathbf{A}\mathbf{m})||_2^2 + \mu ||\mathbf{W}_m \mathbf{m}||_2^2 \qquad (10) \\ &= \phi_d(\mathbf{m}) + \mu \phi_m(\mathbf{m}), \end{aligned}$$

where $\mathbf{W}_d$ are data weights, and $\mathbf{W}_m$ are model weights. We partition the cost function into two components ϕ_d and ϕ_m, with ϕ_d being the data misfit function, and ϕ_m being the model norm function. Finding the minimum of equation 10 results in the normal equations,

$$(\mathbf{A}^H \mathbf{W}_d^H \mathbf{W}_d \mathbf{A} + \mu \mathbf{W}_m^H \mathbf{W}_m)\mathbf{m} = \mathbf{A}^H \mathbf{W}_d^H \mathbf{W}_d \mathbf{d}, \qquad (11)$$

which we solve to find an optimal scattering potential $\mathbf{m} = \mathbf{m}_*$. Then, data can be reconstructed for arbitrary shot locations, and geophones that fall on the nominal grid x_g^n, using the de-migration operator (equation 1). The caveat is that any reconstructed shot gather must have its corresponding common shot image gather sufficiently illuminated by the observed shots.

Key to the construction of $\mathbf{m}_*$, and thus also to the reconstructed data is the choice of the model and data weight matrices, $\mathbf{W}_m$ and $\mathbf{W}_d$. The data weights $\mathbf{W}_d$ is a diagonal matrix that penalizes missing data, such that its i^{th} diagonal element is,

$$[\mathbf{W}_d]_{ii} = \begin{cases} 1 & , \quad i \in \mathscr{I}_d \\ 0 & , \quad i \notin \mathscr{I}_d \end{cases}, \qquad (12)$$

where $\mathscr{I}_d$ is the set of indices corresponding to the observed grid $x_g^{o(q)}$. The construction of model weights is slightly more involved, and draws on the discussion in the previous section. In particular, we define,

$$\mathbf{W}_m = \mathbf{F}^{-1}\mathbf{W}\mathbf{F}, \qquad (13)$$

where $\mathbf{F}$ is the two dimensional Fourier transform over lateral position x_g and depth z. Then, $\mathbf{W}$ is built from a windowing function that penalizes model space alias ($p \neq 0$ in Figure 2). To build the windowing function, we provide some estimate of the bandwidth η of the model space signal, and an estimate of ξ (the maximum dip of the earth's reflectors as parameterized by pseudo-depth and lateral position in the common shot image gather). For example, we could set $\xi = 0$, and $\eta = 2\pi/\Delta x_g^o$, the former for simplicity and the latter motivated by the sampling theorem.

EXAMPLE: SPDR2 FOR EXTRAPOLATION TO NEAR OFFSET TRACES

The successful reconstruction of near offset traces is important to seismic data processing techniques such as surface related multiple elimination (e.g. Ramírez et al., 2006). We use the 6 shot gathers shown in Figure 3, taken from a marine data set from the Gulf of Mexico. Note that we show a subset of the available offsets. The shot gathers have geophones spaced every $26.67m$ with offsets running from $-2.43km$ to $-10.37m$. The shots are spaced every $53.34m$ so that from left to right in Figure 3, the shot location is increasing (see Figure 4a for a schematic representation of the geometry of the first four shot gathers). This is typical of a towed streamer acquisition geometry, and is an important point in constructing an understanding of why SPDR2 can be used to reconstruct near offset traces.

The data in Figure 3a is used by SPDR2 with the goal of reconstructing the first 14 near offset traces for the first ($q = 1$) shot gather, but using information from all six shot gathers in Figure 3a. The argument for this is as follows. If SPDR2 is applied to just the first ($q = 1$) shot gather in Figure 3a, then that part of the model allowing for the reconstruction of near offset traces is not illuminated. If, on the other hand, SPDR2 is applied to the first two shot gathers ($q = 1, 2$), then traces from the second $q = 2$ shot gather will begin to illuminate that part of the model required to reconstruct the near offset traces in the first shot gather. As the third through sixth ($q = 3 \ldots 6$) shot gathers are added to the input data set for SPDR2, the illumination of the pertinent portion of model space is refined. This is illustrated with the schematic in Figure 4. In Figure 4a, the grey filled boxes are the shot locations, and the black filled boxes are the geophone locations on the observed grid $x_g^{o(q)}$. The near offset traces that we want to reconstruct fall between

the shot location and its nearest observed geophone location. In SPDR2, all shot gathers contribute to the construction of the model according to the adjoint operator in equation 2. Hence, in Figure 4b we plot the union of the observed geophone positions from Figure 4a. This represents the lateral locations illuminated in model space, and allows us to suppose that the near offsets for the $q = 1$ shot gather can be recovered via SPDR2. For our example, we illustrate this illumination of model space in Figure 5 where from left to right, we plot $\alpha^{\dagger}(x,z)$ computed using the adjoint (equation 2) and the shot gathers in Figure 3a for, respectively, $n_s = 1 \ldots 6$.

The SPDR2 reconstructed shot gathers are shown in Figure 3c. We expect a good reconstruction result for the first (left most) shot gather, and results that degrade as we increase the shot location q (i.e. as the shot gathers in Figure 3c progress to the right). In Figure 6, we plot the 14 nearest offset traces from the first ($q = 1$) shot gather. In particular, Figure 6a plots the traces from original data (before decimation), and Figure 6b plots the corresponding reconstructed data.

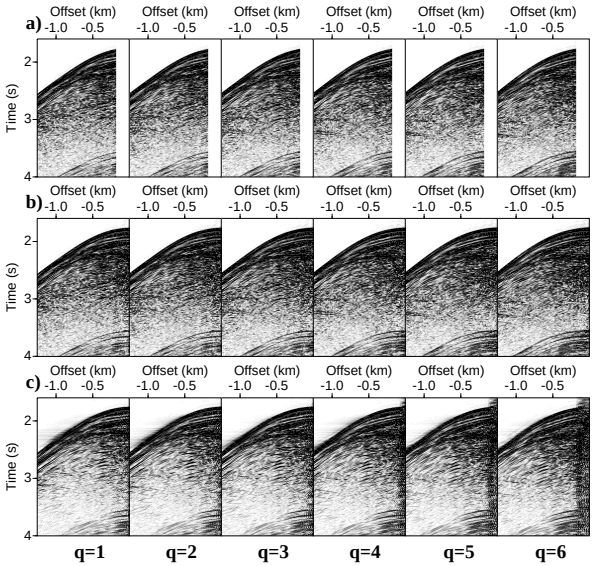

Figure 3: a) The decimated data, b) the original data, c) the reconstructed data computed by applying SPDR2 to the decimated data in a). For plotting purposes, the data are clipped at five percent of their maximum amplitude.

CONCLUSIONS

We introduce two dimensional shot-profile migration data reconstruction (SPDR2). The algorithm, primarily, depends on the use of shot-profile migration image gathers parameterized by lateral position and pseudo-depth. An analysis of SPDR2 shows that they are applicable to earth models consisting of reflectors with limited dip. We illustrated the effectiveness of the algorithm with near offset trace extrapolation for a real data set. We note that the algorithm is equally applicable to data interpolation in both the shot and geophone dimensions.

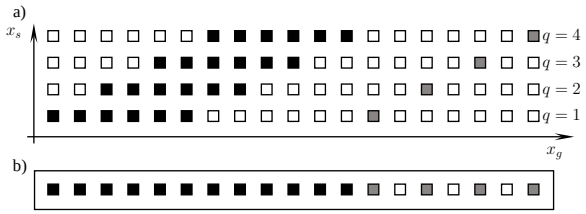

Figure 4: a) We give a schematic representation of the data acquisition for the first four shots. b) We represent the union of the geophone positions for the four shot gathers, and that is representative of the model illumination. We use boxes to represent the nominal grid, black filled boxes to represent the observed grid, and gray filled boxes to represent the shot locations.

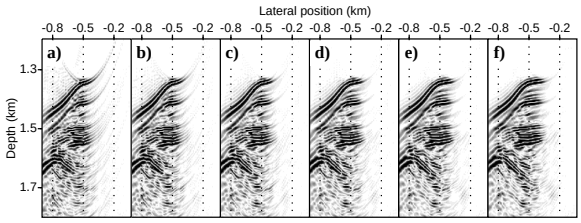

Figure 5: The adjoint computed using the decimated shot gathers in Figure 3a using $n_s = 1 \ldots 6$ shot gathers, so that in a) we show the result for $n_s = 1$ using the $q = 1$ shot gather, and in b) the result for $n_s = 2$ using the $q = 1, 2$ shot gathers, etc.

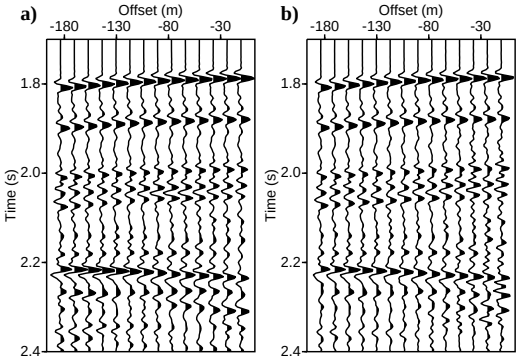

Figure 6: For a small window of time and near offsets, we show a) the original data (before decimation of near offsets), and b) the SPDR2 result obtained from the decimated data (Figure 3a).

EDITED REFERENCES

Note: This reference list is a copy-edited version of the reference list submitted by the author. Reference lists for the 2010 SEG Technical Program Expanded Abstracts have been copy edited so that references provided with the online metadata for each paper will achieve a high degree of linking to cited sources that appear on the Web.

REFERENCES

Biondi, B., 2003, equivalence of source-receiver and shot-profile migration: Geophysics, **68**, 1340–1347. doi:10.1190/1.1598127

Chiu, S. K., and R. Stolt, 2002, Applications of 3-D data mapping – azimuth moveout and acquisition-footprint reduction: 72nd Annual International Meeting, SEG, Expanded Abstracts, 2134–2137.

Clayton, R. W., and R. H. Stolt, 1981, A Born-WKBJ inversion method for acoustic reflection data: Geophysics, **46**, 1559–1567, doi:10.1190/1.1441162.

Gülünay, N., 2003, Seismic trace interpolation in the Fourier transform domain: Geophysics, **68**, 355–369, doi:10.1190/1.1543221.

Hennenfent, G., and F. J. Herrmann, 2006, Seismic denoising with nonuniformly sampled curvelets: Computing in Science & Engineering, **8**, no. 3, 16–25, doi:10.1109/MCSE.2006.49.

Lathi, B. P., 1998, Signal processing and linear systems: Berkeley Cambridge Press.

Liu, B., and M. D. Sacchi, 2004, Minimum weighted norm interpolation of seismic records: Geophysics, **69**, 1560–1568, doi:10.1190/1.1836829.

Naghizadeh, M., and D. Sacchi, 2007, Mutistep autoregressive reconstruction of seismic records: Geophysics, **72**, no. 6, V111–V118, doi:10.1190/1.2771685.

Ramírez, A. C., and A. B. Weglein, 2009, Green's theorem as a comprehensive framework for data reconstruction, regularization, wavefield separation, seismic interferometry, and wavelet estimation: a tutorial: Geophysics, **74**, no. 6, W35–W62, doi:10.1190/1.3237118.

Ramírez, A. C., A. B. Weglein, and K. Hokstad, 2006, Near offset data extrapolation: 76th Annual International Meeting, SEG, Expanded Abstracts, 2554–2558.

Spitz, S., 1991, Seismic trace interpolation in the F-X domain: Geophysics, **56**, 785–794, doi:10.1190/1.1443096.

Stolt, R. H., 2002, Seismic data mapping and reconstruction: Geophysics, **67**, 890–908, doi:10.1190/1.1484532.

Trad, D., 2003, Interpolation and multiple attenuation with migration operators: Geophysics, **68**, 2043–2054, doi:10.1190/1.1635058.